Gas-phase infrared multiple photon dissociation spectroscopy of isolated SF_6^- and SF_5^- anions

Jeffrey D. Steill,[1,2,a)] Jos Oomens,[2] John R. Eyler,[3] and Robert N. Compton[1,4]
[1]*Department of Chemistry, The University of Tennessee, Knoxville, Tennessee 37996-1600, USA*
[2]*FOM Institute for Plasma Physics 'Rijnhuizen', Edisonbaan 14, 3439MN Nieuwegein, The Netherlands*
[3]*Department of Chemistry, The University of Florida, Gainesville, Florida 32611-7200, USA*
[4]*Department of Physics, The University of Tennessee, Knoxville, Tennessee 37996-1200, USA*

(Received 8 August 2008; accepted 6 November 2008; published online 22 December 2008)

Resonantly enhanced multiple photon dissociation of gas-phase SF_6^- and SF_5^- is studied using tunable infrared light from the FELIX free electron laser. The photodissociation spectrum of the sulfur hexafluoride anion, producing SF_5^-, is recorded over the spectral range of 250–1650 cm^{-1}. The infrared multiple photon dissociation cross section exhibits a strong, broad resonance enhancement at 675 cm^{-1} in agreement with the calculated value of ν_3, one of the two IR-active fundamental vibrational modes predicted for the O_h-symmetry ion. Much weaker absorption features are observed in the spectral region of 300–450 cm^{-1} as well as at 580 cm^{-1} that are not easily assigned to the other IR-active fundamental of SF_6^- since these resonances are observed at a much higher energy than the calculated values for the IR-active ν_4 mode. The potential role of binary combination bands is considered. Photodissociation from the sulfur pentafluoride anion produced only F^-, but photodetachment was also observed through SF_6 associative electron capture. The IR multiple photon dissociation spectrum of SF_5^- shows multiple resonances within the region of 400–900 cm^{-1} and agreement with calculations is clear, including the observation of three fundamental frequencies: ν_1 at 780 cm^{-1}, ν_7 at 595 cm^{-1}, and ν_8 at 450 cm^{-1}. Comparisons of the measured frequencies with *ab initio* and density functional theory calculations confirm an SF_5^- anion of C_{4v} symmetry. Similar comparisons for SF_6^- are not inconsistent with an anion of O_h symmetry. © *2008 American Institute of Physics*. [DOI: 10.1063/1.3036977]

I. INTRODUCTION

The sulfur hexafluoride and pentafluoride negative ions are well-studied stable molecular anions that are of practical and fundamental physical interest. SF_6 is a relatively inert, nontoxic, and volatile molecule of great practical utility because it attaches low-energy electrons with a cross section approaching the maximum allowable for *s*-wave capture ($\pi\lambda^2/4\pi^2$).[1] Among many applications, SF_6 is widely employed to increase the dielectric strength of gases (electrical transmission and distribution systems, circuit breakers, etc.), as a plasma etching gas, and in charged particle accelerators. As with all molecules of industrial utility, their environmental impact is of eventual concern. Inadvertent release of SF_6 exhibits a greater global warming potential relative to CO_2 due to its atmospheric stability and very strong infrared (IR) absorption band in a region of the solar spectrum where there are few overlapping atmospheric absorptions. The lifetime of SF_6 in the atmosphere[2] may be determined in part by the reactions of SF_6^- due to the chemical inertness of SF_6. Significant attention has been given to the physical properties of SF_6 due to this practical interest and a review of these properties has been provided by Christophorou and Olthoff.[3,4] There is general agreement upon the experimentally determined properties of SF_6^-, but some significant interest currently exists in resolving discrepancies in reported electron autodetachment lifetimes[5–7] and electron affinities.[8–12]

The SF_6^- anion has also proven to be a challenging molecule for computational investigation. Different methods have produced widely varying results, both for electron affinity and for harmonic frequency values. Density functional theory (DFT) methods have been shown to produce discrepancies in computed molecular structure based upon the functional used.[13] Calculations with certain functionals have produced an interesting feature of the SF_6^- potential energy surface suggesting a global minimum on the potential energy surface of C_{4v} symmetry. The lowest unoccupied molecular orbital of SF_6 is of A_{1g} symmetry so SF_6^- is expected to retain the O_h symmetry of the neutral since this orbital is not degenerate and thus not Jahn–Teller active. An anion structure of lowered symmetry would therefore be unexpected. MP2 methods do not show this tendency to a lower symmetry, as demonstrated by the computations of Gutsev and Bartlett[14] and Miller *et al.*[15] Higher-order *ab initio* harmonic vibrational frequency calculations using coupled-cluster methods including only double excitations (CCD) with the aug-cc-pVDC basis set presented in a study of the electron detachment from metastable SF_6^{-*} also found SF_6^- to be at an O_h minimum.[5] However, as is explored in the current study, this result is basis set dependent for the CCD methods because the C_{4v} minima explored in the DFT calculations of Brinkmann and Schaefer[13] are repeated for certain basis sets. Even between methods that agree upon O_h symmetry struc-

a)Electronic mail: steill@rijnh.nl.

tures, the computed frequency values for the low-energy IR-active ν_4 mode can be quite different. DFT and CCD methods produce a frequency for this vibrational mode that is roughly half that of the MP2 methods.

This disagreement between computational methods has implications beyond spectroscopy; for example, the vibrational frequencies of negative ions obtained from computations are used in models of the dynamics of electron transfer processes in molecules.[5,7,10–12] Results of various computations[5,14,16] of the vibrational frequencies of SF_6^- were used to model the autoionization lifetime of metastable SF_6^{-*}.[5] This model was shown to be very sensitive to the values of the calculated vibrational frequencies, in particular, showing a clear difference between MP2 and other methods. A recent study suggesting a revision of the SF_6 electron affinity from a value of 1.05 eV (Refs. 8 and 9) to 1.2 eV uses MP2 computed frequencies of Gutsev and Bartlett[14] in order to model the electron transfer characteristics.[12] Since modeled equilibria using the molecular anion vibrational density of states are particularly sensitive to magnitudes of the lowest-energy vibrational modes, the vibrational frequency values employed within these models are very important. *Ab initio* and DFT computations are extremely useful for providing reasonable estimates of anion vibrational frequencies; however, experimental constraints upon these values are essential, especially in cases of disagreement between methods. Vibrational spectroscopy is an effective means of determination of structural symmetries and evaluation of harmonic frequency calculations. One method of obtaining information about the vibrational modes of isolated gas-phase ions is through action spectroscopy techniques such as infrared multiple photon dissociation (IRMPD) spectroscopy.[17–19]

There are previous publications regarding experimental observation of the ν_3 vibrational frequency of SF_6^-. A study of Lugez *et al.*[16] obtained a value of 620 cm^{-1} for SF_6^- embedded in a neon matrix. Bopp *et al.*[20] reported observation of the ν_3 frequency of SF_6^- from the IR photodissociation of the $SF_6^-(Ar)_n$ van der Waals complex for $n=1$ and 2. The peak showed a doublet structure that may be related to symmetry-breaking effects due to the Ar atom(s), but a well resolved larger peak allowed for an assignment of the IR-active ν_3 frequency as 683(5) cm^{-1}. Finally, another value based upon experimental data comes from the paper of Borrelli[21] that suggested 680 and 110 cm^{-1} for the ν_3 and ν_4 modes, respectively, based upon the interpretation of the Frank–Condon overlap in the photoelectron spectrum of SF_6^-.[20]

These previous experimental results provide limited means for discrimination between computational methods because the primary source of discrepancy, the ν_4 mode, is not observed and the calculated values of the ν_3 mode are all within the range of a possible spectral shift that might be expected from a matrix-isolated or Ar-tagged measurement. The predicted position of the ν_4 band (100–250 cm^{-1}) makes it difficult to access experimentally, but observation of the ν_3 band for isolated SF_6^- anions might be expected to provide some grounds for assessment of the validity of computational methods. Employing the technique of IRMPD spectroscopy, the current study provides the first experimental gas-phase IR spectrum of isolated SF_6^-. The spectrum is interpreted with the aid of the diverse available computational and experimental results for SF_6^-, and those methods are, in turn, evaluated in the context of the current study. New computational results are presented for SF_6^- and, in particular, the disagreement between MP2 and other methods is examined.

Dissociative electron attachment to SF_6 is well known to produce an abundance of fragment anions.[22] The primary dissociation product from low-energy electron attachment to SF_6 is SF_5^-, which is highly stable relative to the SF_5 radical. SF_5 has a very large electron affinity,[15,23] as much as 3 eV higher than the SF_6 electron affinity of ~1 eV.[8,9] The vibrational spectrum of SF_5^- has been reported as a Cs^+ salt[24] and has also been studied by matrix isolation techniques. Lugez *et al.*[16] reported observations of SF_5^- vibrational frequencies from SF_5^- embedded in a neon matrix, assigned upon the basis of DFT frequency calculations. The current study provides the first isolated gas-phase vibrational spectrum of the SF_5^- anion. The calculation methods employed for SF_6^- are also used to provide novel results for the SF_5^- anion, and these results are used to interpret the IRMPD spectrum. The minimum energy configuration of SF_5^- is unambiguously calculated to be of C_{4v} symmetry in agreement with the calculations of Miller *et al.*[15] and King *et al.*[23] The SF_5^- IRMPD spectrum is observed and, unlike SF_6^-, the major features are all unambiguously assigned to IR-active fundamentals. The dissociation of metastable SF_6^{-*} to produce SF_5^- has been shown to play a competitive role in the determination of the electron autodetachment lifetime.[6,10–12] Spectroscopic investigation of the SF_5^- anion can ultimately be expected to improve the thermodynamic parameters in models of these processes, as well as help evaluate harmonic frequency calculations for SF_6^-.

II. EXPERIMENTAL DETAILS

The experiments were performed by irradiation of ions trapped in a Fourier Transform Ion Cyclotron Resonance (FTICR) mass spectrometer, which is described in detail elsewhere.[25] The SF_6^- ions were generated by electron attachment to SF_6 followed by collisional and radiative stabilization. SF_5^- was formed by low-energy dissociative electron attachment to SF_6. The free electrons were generated with a filament heated by passing a 4.5A current and held at a bias of −90 V relative to ground. The SF_6 source housing was held at a less negative bias of −79 V; thus electrons impacted the SF_6 gas target with approximately 11 eV of energy, but electron attachment occurred from an energy distribution centered at lower energy due to collisional cooling.

The background pressure of 2×10^{-6} torr in the electron ionization source chamber increased with addition of the SF_6 sample to 5×10^{-5} torr. The background pressure was less than 10^{-7} torr in the ion cyclotron resonance (ICR) cell and ion optics region. The ion optics consist of a source region followed by a quadrupole bender and octopole guide into the ICR cell. The ions are stored in the analyzer cell for many seconds and are thus thermally stabilized at approximately room temperature before irradiation. The parent ion of the

species under study is isolated by a stored waveform inverse Fourier transform pulse.[26] A wide range of negative ions is produced from electron collisions with SF_6: F^-, SF_4^-, SF_5^-, and the dominant SF_6^- ion. This wide range of ions is a result of the broad energy distribution of the electron beam. For the SF_6^- experiments, the parent SF_6^- ion was mass selected from the other ions produced before irradiation. For SF_5^-, the initial SF_5^- signal was enhanced by sustained off-resonance rf excitation[27] of SF_6^-, promoting fragmentation to SF_5^-, and then subsequent isolation of the SF_5^- anion prior to IR irradiation.

Dissociation of molecular ions with IR laser radiation from the FELIX (Ref. 28) free electron laser has been described in detail in a thorough review.[18] The bandwidth of the FELIX radiation is transform limited at ~0.5% full width at half maximum of central wavelength (e.g., 3 cm^{-1} at 600 cm^{-1}). The isolated ions were irradiated for 450 ms, corresponding to three FELIX macropulses. Each macropulse was ~5 μs in length and consisted of 5000 micropulses of ~1 ps duration. Four mass spectra were averaged for each wavelength setting to produce a spectral point. Power as a function of wavelength was measured, and the spectra were linearly normalized and wavelength calibrated. Calibrated spectra were averaged over multiple runs to yield the final spectra.

III. COMPUTATIONAL DETAILS

The vibrational frequencies and IR absorption activities as calculated by *ab initio* and DFT methods in concert with previous calculations facilitate interpretation of the IRMPD spectra. Calculations of the predicted vibrational spectra and anion molecular structure are performed with Gaussian Inc.'s GAUSSIAN03 program.[29] Geometry optimizations and frequency calculations are performed with MP2 methods as well as with CCD methods using relatively small to moderate basis sets. The CCD methods are used instead of the more appropriate coupled-cluster method including single, double and perturbative triple excitations (CCSD(T)) and/or the MP4 method including single, double, triple and quadrupole excitations (MP4(SDTQ)) due to limitations of computational resources. These results are compared to the results of earlier studies using DFT,[16,23] MP2,[5,14] and CCD (Ref. 5) methods. The sulfur hexafluoride anion was calculated as a doublet state using unrestricted methods and the sulfur pentafluoride anion was calculated as a singlet state with restricted methods. All *ab initio* optimization and frequency calculations used the frozen-core approximation. The optimization and frequency calculation methods used for the SF_6^- and SF_5^- anions all show less than 10% error in the calculated bond length and vibrational frequencies when applied to the SF_6 neutral, including harmonic frequencies scaled by a factor of 0.95.

IV. RESULTS AND DISCUSSION

A. Dissociation and detachment channels of SF_6^- and SF_5^-

The observed products of IRMPD are in agreement with what would be expected from thermodynamics as the lowest-energy dissociation pathways were observed for each ion. Multiple photon dissociation of SF_6^- resulted primarily in SF_5^-, and irradiation of SF_5^- produced F^- ions. For SF_6^-, the dissociation to SF_5^- is energetically favored over dissociation to F^- by approximately 0.6 eV, with a dissociation energy of approximately 1.6 eV according to G2 and G3 calculations.[15] The energy required for each of these bond dissociation reactions is considerably less than the vertical detachment energy of SF_6^- at approximately 3 eV.[20] According to both DFT and *ab initio* methods, the dissociation energy to produce the SF_4^- and F radicals from SF_5^- is approximately 1–2 eV larger than the dissociation energy of approximately 2.4 eV to produce SF_4 and F^-. The vertical detachment energy of SF_5^- is more than 4 eV according to DFT (Ref. 23) and *ab initio*[15] calculations.

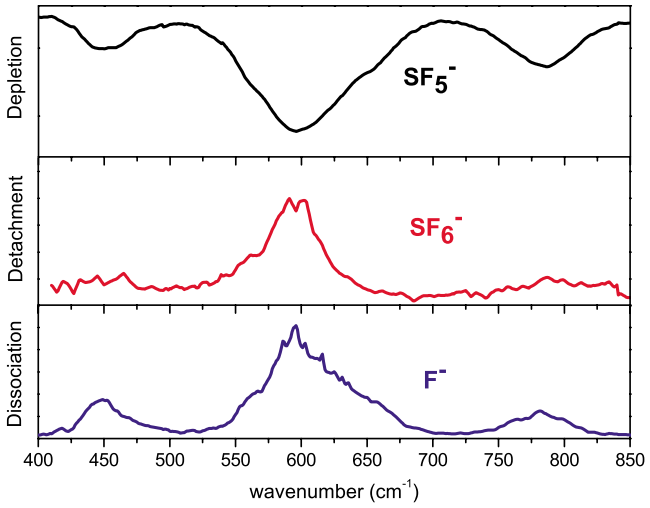

FIG. 1. (Color online) SF_5^- photodetachment (middle) and photodissociation (bottom) spectra. The photodissociation and photodetachment resonances from SF_5^- can be compared to the depletion of the parent ion (top). The SF_6^- appearance spectrum (middle) is due to the electron scavenger behavior of residual SF_6 in the FTICR cell.

The fact that the dissociation energies of SF_6^- and SF_5^- are comparable to the electron affinities suggests that electron detachment from the SF_5^- and SF_6^- anions might compete with the dissociation process. This was observed indirectly for SF_5^- since the depletion of the parent ion signal is found to be greater than the sum of the fragment ion signals observed by photodissociation. SF_5^- autodetachment was also positively identified. As shown in Fig. 1, due to the small amount of background neutral SF_6 in the FTICR cell, free electrons produced from SF_5^- IR photodetachment produce a detectable SF_6^- signal from electron capture that correlates with the IR activity in the SF_5^- spectrum as demonstrated by the dissociation resonances. Photodetachment may also occur for SF_6^-, but this was not necessarily experimentally discernable in the current configuration. The possibility of SF_6^- photodetachment was investigated by addition of CCl_4 background gas to the FTICR cell. Dissociative electron capture to CCl_4 to form Cl^- was not observed, suggesting that the dissociation process may dominate over electron detachment in the present experiment. However, this is only suggestive and not conclusive, as the CCl_4 background pressure was only one order of magnitude larger than the neutral

TABLE I. SF_6^- harmonic frequency calculations, with values scaled by a common factor of 0.95. These calculations are constrained to O_h symmetry. Certain methods produced imaginary frequencies for the ν_4 mode that are shown in boldface. These methods show a minimum energy structure of C_{4v} symmetry. The IR-active modes are of T_{1u} symmetry.

Method/basis	R	$\nu_6(T_{2u})$	$\nu_5(T_{2g})$	$\nu_4(T_{1u})$	$\nu_2(E_g)$	$\nu_1(A_{1g})$	$\nu_3(T_{1u})$
			MP2				
6-311+G(S:2*df*,F:2*d*)[a]	1.716	225	319	291	425	595	686
aug-cc-pVDZ[b]	1.744	221	314	302	456	605	711
6-311+G(S:3*df*,F:2*d*)[b]	1.710	232	323	272	424	606	678
6-311+G(3*df*)[b]	1.709	229	323	265	422	602	673
			CCD				
6-311+G*[c]	1.728			189*i*			
6-311+G(S:2*d*,F:*d*)[c]	1.733			92*i*			
aug-cc-pVDZ[b]	1.734	227	319	135	474	607	678
			Hybrid-DFT				
B3LYP/DZP++[d]	1.744	220	319	113	432	580	640

[a]Gutsev and Bartlett (Ref. 14).
[b]Cannon *et al.* (Ref. 5).
[c]Current work.
[d]Lugez *et al.* (Ref. 16).

SF_6 background pressure, perhaps too low to overcome the greater efficiency of SF_6 toward low-energy electron capture. Nonetheless, the failure to observe SF_6^- autodetachment leading to dissociative electron attachment to CCl_4 is not inconsistent with recent work regarding the competition between these two processes. The studies of Troe *et al.*[11] and Graupner[6] *et al.* showed that the rate of dissociation effectively competes with that of detachment when the internal energy of the ion is greater than the dissociation threshold of approximately 1.6 eV. Application of a model for the multiple photon IR excitation dynamics[18] suggests a mean energy of ~2 eV for the excited SF_6^- anion. One could thus interpret the lack of indirect SF_6^- photodetachment signal as indicative of dissociation dominating over detachment.

B. SF_6^- observed and calculated spectra: Spectral assignments

Harmonic vibrational frequencies resulting from *ab initio* and DFT computations for SF_6^- constrained to O_h symmetry are shown in Table I. Examination of this table reveals that there is an overall agreement between the different methods employed.[5,14,16] In general, however, the MP2 results differ from the DFT and CCD results with regard to the ν_3 and especially the ν_4 mode. The CCD method is expected to improve upon the MP2 results, but with some basis sets of moderate size, such as 6-311+G(S:2*d*,F:*d*), the CCD method produces imaginary frequencies at O_h geometries and optimizes to the lowered symmetry explored by Brinkmann and Schaefer.[13] This result would seem likely to be an artifact because when the aug-cc-pVDZ basis is used with these same methods the expected O_h structure is produced.[5] MP2 methods do not produce this feature regardless of the basis set employed; increasing the basis set size for the MP2 calculations does not produce any significant shift of predicted frequencies, only a slight reduction in the values of the ν_3 and ν_4 frequencies. This disagreement among the methods for the frequency of the lowest-energy T_{1u} mode, ν_4, is related to the issue of lowered symmetry. Essentially, the discrepancy among calculations pertaining to the ν_4 mode extends even to the direction of curvature of the potential energy surface. This might suggest that the CCD method is suspect as employed for this anion. In particular, the use of CCD methods instead of CCSD(T) may be particularly problematic due to the lack of inclusion of triple excitations. MP4(SDQ) harmonic frequency calculations show the same strong basis set dependence as the CCD frequency calculations and the importance of triple excitations in the MP4(SDTQ) method has been demonstrated.[30] The SF_6^- calculations of the current study therefore do not add to the previously published calculations for purposes of spectral interpretation, and in fact suggest some degree caution regarding the previous computational results. Nonetheless, while it is clear that further theoretical work regarding the SF_6^- potential energy surface is required, the available calculations shown in Table I do provide a sufficient basis for spectral interpretation.

The CCD/aug-cc-pVDZ and DFT results show a dramatic decrease of the ν_4 frequency compared to the MP2 results, with MP2 methods predicting a band above 250 cm^{-1}, and DFT and CCD calculations always falling well below 150 cm^{-1}. This is the main point of difference between the methods, although there is also a tendency for the MP2 methods to predict a moderately larger value for the ν_3 mode. While the largest point of difference between the MP2 and the other methods is thus on the edge of spectral range of the current study, sufficient difference also exists in the predicted positions of the ν_3 fundamental to facilitate evaluation between these calculation methods.

The IRMPD spectrum of SF_6^- is shown in Fig. 2. Based on comparison with the calculated frequencies in Table I, the large peak with a maximum at 675 cm^{-1} is interpreted as the ν_3 mode of SF_6^-. This gas-phase value compares favorably

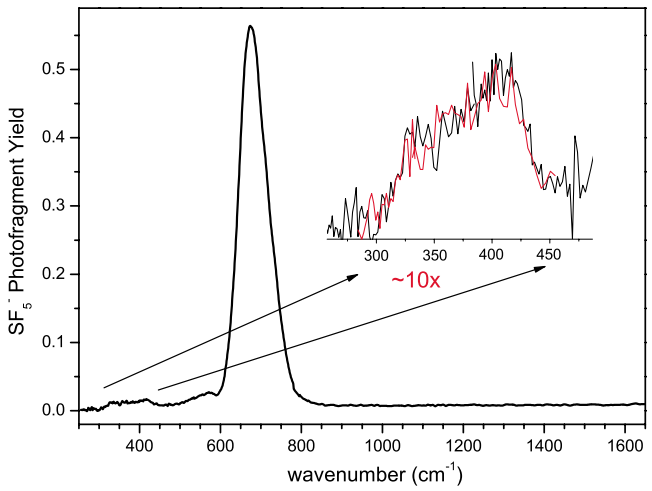

FIG. 2. (Color online) Observed SF_6^- IRMPD spectrum. Abundance of the SF_5^- photoproduct, which peaks at 675 cm^{-1}, is plotted vs laser wavelength. The spectrum shown is the average of multiple runs. The inset shows two independent runs over the unassigned spectral feature at lower wavenumbers.

with the value of 683(5) cm^{-1} reported recently by Bopp *et al.*[20] using the Ar-tagging method. It is considerably higher than the value of 620 cm^{-1} obtained by Lugez *et al.*[16] for SF_6^- embedded in a neon matrix. The calculated frequencies for this mode roughly agree within the methods and with the data, so this low-resolution assignment is unambiguous. The doublet structure of this band reported in the Ar-tagged spectrum by Bopp *et al.*[20] was not observed. It is possible that the width of the IRMPD band may obscure this feature. It is also possible that this splitting is not an inherent feature of the SF_6^- anion, but is induced by perturbations from the rare-gas atom. It is noteworthy that the center of the peaks observed in the Ar-tagged spectrum of Bopp *et al.*[20] is quite close to the band center of the data presented in Fig. 2.

Left unscaled, the calculated frequencies for the ν_3 mode are too large, but application of a common scaling factor of 0.95 to the *ab initio* calculations gives an improved comparison, yielding a value of 686 cm^{-1} for the MP2 calculation of Gutsev and Bartlett[14] and 677 cm^{-1} for the CCD/aug-cc-pVDZ (Ref. 5) calculation. The CCD/aug-cc-pVDZ calculation produces a closer match for this band than the MP2 calculations of the same basis set size. However, scaled MP2 calculations using larger basis sets resulted in lowered values for the ν_3 and ν_4 modes. For example, the MP2/6-311 +G(3*df*) calculation produces an improved scaled frequency value of 673 cm^{-1} for the ν_3 mode.

Aside from the main absorption band at 675 cm^{-1}, additional features are observed at 400 and 580 cm^{-1} in the experimental spectrum, but none of the O_h-symmetry calculations predict an IR-active fundamental within 100 cm^{-1} of this range. The lowest-energy band is not easily assignable to the IR-active fundamental of the ν_4 mode, which is the main point of difference between the different computational methods. MP2 methods unanimously suggest a frequency in the range of 250–300 cm^{-1}, and CCD and DFT methods suggest a vibrational frequency of approximately half this value or less. Thus, both resonances are too high in energy to be interpreted as arising from the other IR-active SF_6^- fundamental vibration. There is no sign of an absorption feature at the far red edge of the spectrum, 250 cm^{-1}, where experimental constraints did not permit investigation at longer wavelengths. Like the SF_6 neutral, SF_6^- is expected to show a much stronger absorption cross section for the ν_3 mode as compared to the ν_4 mode. Thus, it is possible that this band is weak, but dissociation to SF_5^- is facile enough that it is reasonable to suggest the ν_4 band must be at a frequency lower than 250 cm^{-1}, especially considering the width of the observed spectral features.

TABLE II. Symmetry-allowed SF_6^- binary combination bands calculated according to various methods. The wavenumber values are calculated by using the harmonic frequency results for the fundamentals. *Ab initio* results are scaled by a factor of 0.95 and DFT results by 0.98.

Band	Symmetry	MP2[a]	DFT[b]	CCD/aug-cc-pVDZ[c]
$\nu_3-\nu_1$	$A_{1g}\otimes T_{1u}$	96	60	71
$\nu_5-\nu_6$	$T_{2g}\otimes T_{2u}$	99	99	92
$\nu_5-\nu_4$	$T_{2g}\otimes T_{1u}$	30	206	184
$\nu_3-\nu_2$	$E_g\otimes T_{1u}$	275	208	204
$\nu_2-\nu_6$	$E_g\otimes T_{2u}$	210	212	247
$\nu_2-\nu_4$	$E_g\otimes T_{1u}$	141	319	339
$\nu_3-\nu_5$	$T_{2g}\otimes T_{1u}$	386	321	359
$\nu_1-\nu_4$	$A_{1g}\otimes T_{1u}$	320	467	472
$\nu_5+\nu_4$	$T_{2g}\otimes T_{1u}$	642	432	454
$\nu_5+\nu_6$	$T_{2g}\otimes T_{2u}$	573	539	546
$\nu_2+\nu_4$	$E_g\otimes T_{1u}$	753	545	609
$\nu_2+\nu_6$	$E_g\otimes T_{2u}$	684	652	701
$\nu_1+\nu_4$	$A_{1g}\otimes T_{1u}$	932	693	742
$\nu_3+\nu_5$	$T_{2g}\otimes T_{1u}$	1058	959	998
$\nu_3+\nu_2$	$E_g\otimes T_{1u}$	1169	1072	1152
$\nu_3+\nu_1$	$A_{1g}\otimes T_{1u}$	1348	1220	1285

[a]Gutsev and Bartlett (Ref. 14).
[b]Lugez *et al.* (Ref. 16).
[c]Cannon *et al.* (Ref. 5).

The absorptions in the region between 300 and 600 cm^{-1} may be due to combination bands, which play a significant role in the SF_6 neutral IR spectrum.[31] Assuming the SF_6^- anion is of O_h symmetry such as the parent neutral, the symmetry-allowed binary combination bands are surprisingly few. IR-active combination bands must contain the T_{1u} representation within the symmetry product. From the symmetry direct product table of the O_h point group[32] it is determined that the binary combinations that contain this representation are $A_{1g}\otimes T_{1u}$, $E_g\otimes T_{1u}$, $E_g\otimes T_{2u}$, $T_{2g}\otimes T_{1u}$, and $T_{2g}\otimes T_{2u}$. Table II lists the possible combination bands, their symmetries, and predicted harmonic energies.

Upon examination of Table II, the low-energy resonance at 400 cm^{-1} is interpretable as arising from various possible candidates such as the $\nu_1-\nu_4$ difference band, the $\nu_5+\nu_4$ band, and/or the $\nu_3-\nu_5$ band. The SF_6 neutral shows a significant activity for the $\nu_1\pm\nu_4$ bands,[31] and thus its anion of same symmetry might be expected to do so as well, especially considering the high populations of excited vibrational states present in the low-frequency ν_4 mode even at room temperature. Like the SF_6 neutral, there are symmetry-allowed binary combination bands in the same spectral region as the ν_3 fundamental. The large width of the main absorption feature may also be due in part to contributions

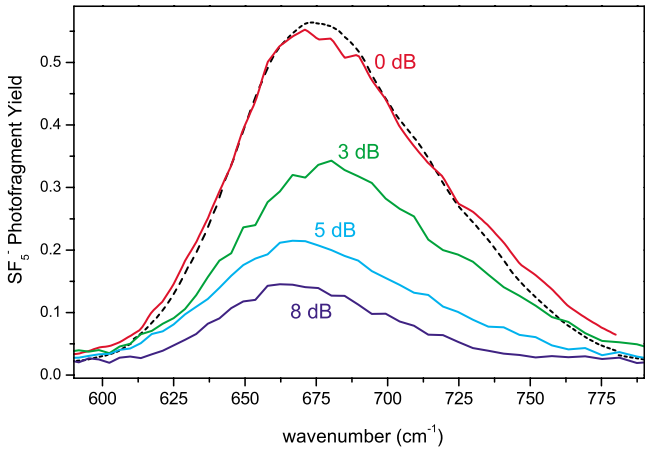

FIG. 3. (Color online) Attenuated SF_6^- IRMPD spectra. Abundance of the SF_5^- photoproduct is plotted vs laser wavelength at varying degrees of laser attenuation. The spectrum shown as a dotted line is the average of multiple full-power runs.

from potentially interfering combination bands such as $\nu_1+\nu_4$ and/or $\nu_2+\nu_6$. The failure to observe any combination bands to the far high-energy side of the ν_3 fundamental suggests that some degree of caution should be used in applying this interpretation, but IRMPD experiments often show enhancement of IR activity on bands to the low-energy side of a strong band.[18] This is because absorption is enhanced due to the strong band slowly shifting into resonance as the ion becomes energized, as a consequence of the anharmonicity of the potential.

The close agreement of the scaled MP2/6-311+G(3*df*) harmonic frequency calculations to the observed value of the ν_3 vibrational mode is at odds with the failure to observe the predicted ν_4 band at energies above 250 cm^{-1}. This suggests that the DFT and CCD results are more accurate in regard to the lower value for the ν_4 vibrational mode. Thus, the best overall agreement for spectral interpretation is obtained using the scaled CCD/aug-cc-pVDZ calculation with values of 678 and 135 cm^{-1} for the ν_3 and ν_4 modes, respectively. This interpretation is supported by the photoelectron spectrum Frank–Condon analysis of Borrelli[21] that predicts a value of 680 cm^{-1} for the ν_3 mode and simultaneously suggests a value of 110 cm^{-1} for the ν_4 mode of SF_6^-.

C. SF_6^- observed spectrum: Spectral peak width

The extreme width of the ν_3 SF_6^- band is striking, and the effect of laser power is examined to determine if it is an inherent feature of the band. As shown in Fig. 3, measurements at lower laser power gave somewhat narrower IRMPD peaks. The very small redshift observed at lower laser pulse energies is probably caused by the fact that at lower laser powers only the hottest wing of the Boltzmann distribution is excited to above the dissociation threshold; these hotter molecules are slightly more influenced by anharmonicity explaining the slight redshift. The broadening persists despite a much reduced power, and thus appears not to be a saturation effect. The source of this broadening is also not expected to result from internally "hot" ions since there is a delay on the order of seconds from the time of SF_6^- formation to laser irradiation, and thus it is expected that the anions are collisionally and/or radiatively thermalized to room temperature. Using an electrospray ionization source, we have reported IRMPD anion spectra with much narrower bandwidths[33] so that the broadening is not an inherent feature of anion IRMPD spectra. It is known that the degree of vibrational anharmonicity is a factor in the broadening of IRMPD band profiles.[18] In addition, potentially interfering combination bands such as the symmetry-allowed $\nu_1+\nu_4$ are predicted in the spectral region. This would mean that the increased bandwidth is an inherent property of this particular species as probed by IRMPD spectroscopy, and does not necessarily conceal well-defined observable structure. The peak maximum of the unattenuated scans is reported as the ν_3 peak position because this value is highly reproducible, as shown in the comparison of the unattenuated 0 dB single scan to the average of multiple runs in Fig. 3.

D. SF_5^- observed and calculated spectra: Spectral assignments

There is no ambiguity in the general symmetry of the calculated structure and for the vibrational frequencies of the

TABLE III. SF_5^- harmonic frequencies (in cm^{-1}) scaled by 0.95 for *ab initio* methods and 0.98 for DFT methods. Calculations are constrained to C_{4v} symmetry.

Mode	ν_9	ν_6	ν_4	ν_3	ν_8	ν_5	ν_2	ν_7	ν_1
Symmetry	E	B_2	B_1	A_1	E	B_2	A_1	E	A_1
				MP2					
aug-cc-pVDZ	219	219	292	392	406	421	485	610	735
aug-cc-pV(S:TZ,F:DZ)	227	240	310	411	431	399	485	583	745
				CCD					
6-311+G*	223	247	313	427	442	411	496	586	747
6-311+G(S:2*df*,F:2*d*)	237	259	330	444	464	430	516	607	781
aug-cc-pVDZ	227	237	307	426	432	447	509	623	773
aug-cc-p(S:TZ, F:DZ)	238	258	327	427	442	459	513	601	781
				Hybrid-DFT					
B3LYP/DZP++[a]	215	225	297	404	416	398	482	589	756
Expt. (current work)					450			595	780

[a]Lugez *et al.* (Ref. 16).

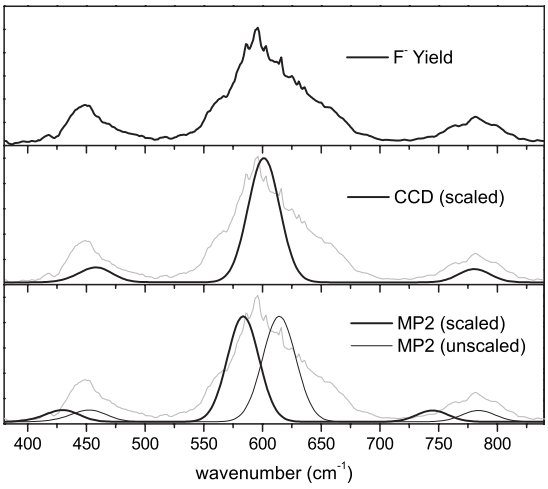

FIG. 4. Observed and calculated SF_5^- spectra. The top panel shows abundance of the F^- photoproduct plotted vs laser wavelength and the lower panels show simulated SF_5^- IR absorption spectra overlaid with the experimental data. Both calculations shown use the aug-cc-pV(S:TZ,F:DZ) basis set. Calculated frequencies are scaled by 0.95. The MP2 calculation is also shown unscaled.

SF_5^- anion. All computational methods give rough agreement, as shown in Table III. The vibrational frequencies of SF_5^- are calculated by methods similar to SF_6^-. The MP2 and CCD calculations of the SF_5^- anion structure and frequencies are in relative agreement and unanimously predict an ion of C_{4v} symmetry that is similar in structure to the DFT studies of King *et al.*[23] Unlike SF_6^-, there are no extreme differences between calculations for any of the frequency values of the vibrational modes of SF_5^-.

The predicted vibrational spectra of SF_5^- calculated by MP2 and CCD methods with the aug-cc-pV(S:TZ,F:DZ) basis set (aug-cc-pVDZ on the fluorine atoms and aug-cc-pVTZ on the sulfur atom) are shown in Fig. 4. As is the case for SF_6^-, comparison of the predicted spectra with the observed spectrum allows for an assessment of the quality of the various calculation methods employed. For visual comparison the predicted and observed SF_5^- IR spectra are stacked in Fig. 4.

The IR wavelength dependence of the dissociation of SF_5^- into F^- showed at the top panel of Fig. 4 reveals multiple bands that are well resolved. The resonances in the IRMPD spectrum of the SF_5^- anion at 780, 595, and 450 cm^{-1} are consistent with the predicted positions and intensities for the ν_1, ν_7, and ν_8 fundamentals, respectively. These values compare reasonably to those observed by previous studies such as the Cs^+ salt spectrum[24] peaks at 793, 590, and 466 cm^{-1}, and the Ne matrix isolation spectrum[16] assignments of 795, 603, and 470 cm^{-1}. The unperturbed gas-phase frequencies show that the matrix and solid-phase spectra slightly blueshift the ν_1 and ν_8 bands. As shown in the middle panel of Fig. 4, the best agreement is obtained with the scaled CCD/aug-cc-pV(S:TZ,F:DZ) calculation. The MP2 results with the same basis set, as shown in the bottom panel of Fig. 4, do not give entirely satisfactory agreement with or without an applied scaling factor.

V. CONCLUSIONS

Analysis of the IRMPD spectra in terms of the computational results provides a confident assignment of the observed SF_5^- anion spectrum and a reasonable assignment of the SF_6^- spectrum. The major feature of the SF_6^- spectrum is assigned unambiguously to the ν_3 fundamental band, in agreement with the work of Bopp *et al.*[20] and Borelli,[21] confirming the presence of an anion of O_h symmetry. The peak shown in Figs. 2 and 3 does not appear to be split into a multiplet structure as reported in the Ar-tagging results of Bopp *et al.*,[20] but the peak is sufficiently broadened that this structure may be obscured.

The present results provide an experimental benchmark for a molecular anion of considerable interest that has proven to be difficult to model computationally. The disagreement between MP2 and other methods is not fully resolved, but the failure to observe any IR absorptions from the ν_4 band in the range of 250 cm^{-1} suggest that the DFT and CCD methods are possibly more accurate in predicting the value of the lowest vibrational frequency of SF_6^-. This interpretation is in agreement with the Frank–Condon analysis of the SF_6^- photoelectron spectrum[20] of Borelli,[21] and has important implications for models of SF_6^- electron transfer employing anion densities of states as parameters.

The IR spectrum of SF_5^- is observed and confidently interpreted on the basis of novel computations. The calculated symmetry and therefore structural characteristics are confirmed, and based upon comparison to the IR dissociation spectrum, the scaled frequencies of the CCD/aug-cc-pV(S:TZ,F:DZ) calculation are shown to provide a good computational model for the SF_5^- anion. The matrix-isolated[16] and $Cs^+SF_5^-$ salt[24] spectra are shown to be slightly blueshifted relative to the gas-phase spectral bands. In addition to the SF_5^- dissociation spectrum, the well-known electron attachment behavior of SF_6 has been demonstrated to provide a means for detection of SF_5^- photodetachment. The use of SF_6 and other molecules with large low-energy electron attachment cross sections for this type of low-energy free electron detection is commonly referred to as the SF_6 scavenger technique and has also been successfully employed to observe electronic and transient negative ion states in many electron scattering studies as discussed in a recent review.[34] This observation of IR multiple photon photodetachment from SF_5^- using the SF_6 electron scavenger is worthy of further investigation since it has the potential to be developed into an effective form of IR action spectroscopy of gas-phase negative ions for which the photodetachment process competes with photodissociation. These methods have been employed previously[35] using CCl_4 as the electron capture molecule, although not with a free electron laser and not with the same success in correlating detachment and dissociation resonances.

ACKNOWLEDGMENTS

We thank Dr. Boris Sartakov for modeling of the SF_6^- dissociation dynamics and for helpful discussions regarding the SF_6^- potential energy surface. The authors would also like to thank the FELIX staff, particularly Dr. B. Redlich and

Dr. A.F. G. van der Meer, for their excellent support. This work is part of the research program of FOM, which is financially supported by the Nederlandse Organisatie voor Wetenschappelijk Onderzoek (NWO). R.N.C. gratefully acknowledges financial support provided by the National Science Foundation (No. CHE-0352398), and we also gratefully acknowledge additional travel funding provided by the NSF-sponsored High Field FTICR Facility at the National High Magnetic Field Laboratory in Tallahassee, Florida.

[1] R. N. Compton, L. G. Christophorou, G. S. Hurst, and P. W. Reinhardt, J. Chem. Phys. **45**, 4634 (1966).
[2] R. A. Morris, T. M. Miller, A. A. Viggiano, J. F. Paulson, S. Solomon, and G. Reid, J. Geophys. Res., [Atmos.] **100**, 1287 (1995).
[3] L. G. Christophorou and J. K. Olthoff, J. Phys. Chem. Ref. Data **29**, 267 (2000).
[4] L. G. Christophorou and J. K. Olthoff, Int. J. Mass Spectrom. **205**, 27 (2001).
[5] M. Cannon, Y. Liu, L. Suess, F. B. Dunning, J. D. Steill, and R. N. Compton, J. Chem. Phys. **127**, 064314 (2007).
[6] K. Graupner, T. A. Field, A. Mauracher, P. Scheier, A. Bacher, S. Denifl, F. Zappa, and T. D. Märk, J. Chem. Phys. **128**, 104304 (2008).
[7] J. Rajput, L. Lamich, and L. Andersen, Phys. Rev. Lett. **100**, 153001 (2008).
[8] E. P. Grimsrud, S. Chowdhury, and P. Kebarle, J. Chem. Phys. **83**, 1059 (1985).
[9] G. E. Streit, J. Chem. Phys. **77**, 826 (1982).
[10] J. Troe, T. M. Miller, and A. Viggiano, J. Chem. Phys. **127**, 244303 (2007).
[11] J. Troe, T. M. Miller, and A. Viggiano, J. Chem. Phys. **127**, 244304 (2007).
[12] A. Viggiano, T. M. Miller, J. F. Friedman, and J. Troe, J. Chem. Phys. **127**, 244305 (2007).
[13] N. R. Brinkmann and H. F. Schaefer, Chem. Phys. Lett. **381**, 123 (2003).
[14] G. L. Gutsev and R. J. Bartlett, Mol. Phys. **94**, 121 (1998).
[15] T. M. Miller, S. T. Arnold, and A. A. Viggiano, Int. J. Mass Spectrom. **227**, 413 (2003).
[16] C. L. Lugez, M. E. Jacox, R. A. King, and H. F. Schaefer, J. Chem. Phys. **108**, 9639 (1998).
[17] M. A. Duncan, Int. J. Mass Spectrom. **200**, 545 (2000).
[18] J. Oomens, B. G. Sartakov, G. Meijer, and G. von Helden, Int. J. Mass Spectrom. **254**, 1 (2006).
[19] L. MacAleese and P. Maître, Mass Spectrom. Rev. **26**, 583 (2007).
[20] J. C. Bopp, J. R. Roscioli, M. A. Johnson, T. M. Miller, A. A. Viggiano, S. M. Villano, S. W. Wren, and W. C. Lineberger, J. Phys. Chem. A **111**, 1214 (2007).
[21] R. Borrelli, Chem. Phys. Lett. **445**, 84 (2007).
[22] M. Braun, S. Barsotti, S. Marienfeld, E. Leber, J. M. Weber, M.-W. Ruf, and H. Hotop, Eur. Phys. J. D **35**, 177 (2005).
[23] R. A. King, J. M. Galbraith, and H. F. Schaefer, J. Phys. Chem. **100**, 6061 (1996).
[24] K. O. Christe, E. C. Curtis, C. J. Schack, and D. Pilipovich, Inorg. Chem. **11**, 1679 (1972).
[25] J. J. Valle, J. R. Eyler, J. Oomens, D. T. Moore, A. F. G. van der Meer, G. von Helden, G. Meijer, C. L. Hendrickson, A. G. Marshall, and G. T. Blakney, Rev. Sci. Instrum. **76**, 023103 (2005).
[26] A. G. Marshall, T. C. Wang, and T. L. Ricca, J. Am. Chem. Soc. **107**, 7893 (1985).
[27] J. W. Gauthier, T. R. Trautman, and D. B. Jacobson, Anal. Chim. Acta **246**, 211 (1991).
[28] D. Oepts, A. F. G. van der Meer, and P. W. van Amersfoort, Infrared Phys. Technol. **36**, 297 (1995).
[29] M. J. Frisch, G. W. Trucks, H. B. Schlegel *et al.*, GAUSSIAN03, Revision C.02, Gaussian, Inc., Wallingford, CT, 2004.
[30] W. Wang, W. Zheng, X. Pu, N.-B. Wong, and A. Tian, J. Mol. Struct.: THEOCHEM **625**, 25 (2003).
[31] R. S. McDowell, B. J. Krohn, H. Flicker, and M. C. Vasquez, Spectrochim. Acta, Part A **42**, 351 (1986).
[32] D. C. Harris and M. B. Bertolucci, *Symmetry and Spectroscopy* (Dover, New York, 1989).
[33] J. Oomens and J. D. Steill, J. Phys. Chem. A **112**, 3281 (2008).
[34] N. Mirsaleh-Kohan, W. D. Robertson, and R. N. Compton, Mass Spectrom. Rev. **27**, 237 (2008).
[35] R. N. Rosenfeld, J. M. Jasinski, and J. I. Brauman, J. Chem. Phys. **71**, 1030 (1979).